

ORIGINAL ARTICLE

Influence of spacer length on liquid crystal microstructures of branched polyethyleneimines with mesogenic pendent groups

Seiji Ujiie¹, Wataru Miyazaki² and Kazuyoshi Iimura²

Side-chain liquid crystal polyethyleneimines (PEI; P-*n*) with different spacer lengths (*n*) were synthesized, and their thermal and liquid crystalline properties were examined. The P-*n* polymers showed liquid-crystalline phases upon heating and cooling. P-*n* with a short methylene spacer (*n* = 2–5) formed a smectic A (SmA₂) phase with a bilayered structure. However, P-*n* with a longer methylene spacer than a pentamethylene chain (*n* = 6–12) exhibited a smectic A (SmA₁) phase with a monolayered structure. P-2, P-3 and P-4 showed only the SmA₂ phase. P-*n* with *n* = 5–9 revealed a nematic phase and the smectic A phase. P-8 and P-9 displayed smectic C and F phases, as well as the SmA₁ and nematic phases. P-10, P-11 and P-12 exhibited SmA₁ and smectic F phases. These results indicate that the microstructures of the liquid crystalline phases depend on the balance between the spacer length and the length of the mesogenic group containing the terminal unit. This is useful information for the design of side-chain liquid crystal polymers.

Polymer Journal (2012) 44, 561–566; doi:10.1038/pj.2012.64; published online 18 April 2012

Keywords: flexible spacer; liquid crystal formation; liquid crystal polymer; mesogenic pendent; orientational behavior; phase transition; polyethyleneimine

INTRODUCTION

Research on new liquid crystalline materials is important from both scientific and technological viewpoints. Understanding the relationship between the chemical structures and physicochemical properties is useful for the design of liquid crystalline materials.^{1–8} It is well known that the liquid crystal formation in side-chain liquid crystal polymers generally depends on structural factors such as the spacers and polymer backbones.^{1–4,9} Various studies on side-chain liquid crystal polymers progressed after the concept of flexible spacers was proposed.¹⁰ A methylene chain is usually used as the flexible spacer, which is linked to a skeletal main chain with mesogenic units. In general, an increase in the spacer length can enhance liquid crystal formation in side-chain liquid crystal polymers. The effects of the spacer chain length have been reported for side-chain liquid crystal polymers with polymer backbones, such as polysiloxane, polyacrylate and polymethacrylate. We previously described the synthesis of side-chain liquid crystal polymers through the reaction of branched polyethyleneimine (PEI) and aromatic-mesogenic groups with bromoalkyl units. Their thermal and liquid crystalline properties were examined, and the formation of nematic and smectic phases in the side-chain liquid crystal polymers was reported.¹¹ In this PEI system, the relationship between the spacer chain length and liquid crystalline properties was not clearly investigated. In a series of related

studies, however, we found that side-chain liquid crystal polymers with short spacers exhibited higher smectic formation abilities than those with long spacers. To investigate the influence of the spacer chain length in detail, we synthesized side-chain liquid crystal polymers with branched PEI backbones and examined their thermal and liquid crystalline properties. The relationship between the liquid crystalline properties and the spacer length in the side-chain liquid crystal PEIs with branched structures was demonstrated. This paper describes the liquid crystal formation and liquid crystalline properties of side-chain liquid crystal PEIs that possess mesogenic side groups with spacer chains of different lengths. The results presented can be used for the effective design of liquid crystal polymers.

EXPERIMENTAL PROCEDURE

Materials

The synthesis of the side-chain liquid crystal polymers was performed by modifying a method described in the literature.^{11,12} The liquid crystal polymers were synthesized by the reaction of branched PEI with ω -bromo- α -(4-(4-(butyl)phenylazo)phenoxy)alkane. The branched PEI has primary, secondary and tertiary amino groups. ω -Bromo- α -(4-(4-(butyl)phenylazo)phenoxy)alkane was synthesized by the reaction of α,ω -dibromoalkane and 4-(4-(butyl)phenylazo)phenol. The main synthetic methods are described in the following sections.

¹Department of Applied Chemistry, Faculty of Engineering, Oita University, Oita, Japan and ²Department of Chemistry, Faculty of Science, Science University of Tokyo, Tokyo, Japan

Correspondence: Professor S Ujiie, Department of Applied Chemistry, Faculty of Engineering, Oita University, Dannoharu, Oita 870-1192, Japan.

E-mail: seujiie@oita-u.ac.jp

Received 29 December 2011; revised 22 February 2012; accepted 7 March 2012; published online 18 April 2012

4'-Hydroxy-4-butylazobenzene

4-Butylaniline was dissolved in hydrochloric acid, and the solution was cooled to below 5 °C. For the diazotization, a small amount of sodium nitrite was added at a temperature below 5 °C. A mixture of sodium hydroxide solution and phenol was added to the cooled solution. The reaction mixture was stirred for 1 h at approximately 5 °C, after which the reaction mixture was acidified with concentrated hydrochloric acid. The precipitate was isolated by filtration and dried.

6-Bromo-1-(4-(4-butylphenylazo)phenoxy)hexane

4'-Hydroxy-4-butylazobenzene was dissolved in acetone, and potassium carbonate and 1,6-dibromohexane were added. The reaction mixture was heated at reflux for 100 h. The precipitated potassium bromide was removed by filtration, and the filtrate was evaporated under reduced pressure. Chloroform was added to the crude product, and the chloroform solution was extracted 10 times with water and evaporated. The product was recrystallized from a hexane solution. $^1\text{H NMR}$ (CDCl_3): $\delta = 0.95$ (t, $J = 7.0$ Hz, 3H, $-\text{CH}_3$), 1.5 (m, 12H, $-\text{CH}_2-$), 2.7 (t, $J = 7.0$ Hz, 2H, phenyl- CH_2-), 3.5 (t, $J = 6.5$ Hz, 2H, Br- CH_2-), 4.0 (t, $J = 6.5$ Hz, 2H, $-\text{OCH}_2-$), 7.0 (d, $J = 9.0$ Hz, 2H, phenyl), 7.3 (d, $J = 9.0$ Hz, 2H, phenyl), 8.0 (dd, $J = 18.8$ Hz, $J = 3.0$ Hz, 4H, phenyl).

Liquid crystalline polyamine (P-6) with hexamethylene spacer

P-6 was prepared by the addition reaction of branched PEI (molecular weight = 1200 (DP = 28)) with 6-bromo-1-(4-(4-butylphenylazo)phenoxy)hexane (Figure 1). PEI and 6-bromo-1-(4-(4-butylphenylazo)phenoxy)hexane were dissolved in a mixed solution of tetrahydrofuran and acetonitrile. Potassium carbonate was added to the reaction mixture, and the reaction mixture was heated at reflux for 400 h. After the reaction, the mixture was evaporated. The crude product was dissolved in tetrahydrofuran, and the PEI with the butylazobenzene mesogenic groups (P-6) was reprecipitated by the addition of hexane. $^1\text{H NMR}$ (CDCl_3): $\delta = 0.86$ (t, $J = 7.2$ Hz, 3H, $-\text{CH}_3$), 1.36 (m, 12H, $-\text{CH}_2-$), 2.56 (m, 6H, $-\text{NCH}_2-$, 2H, phenyl- CH_2-), 3.88 (m, 2H, $-\text{OCH}_2-$), 6.82 (d, $J = 11.4$ Hz, 2H, phenyl), 7.2 (d, $J = 11.4$ Hz, 2H, phenyl), 7.78 (dd, $J = 14.3$ Hz, $J = 4.3$ Hz, 4H, phenyl). The other side-chain liquid crystal PEIs (P- n , Figure 1) were synthesized using the same method.

Measurements

$^1\text{H NMR}$ measurements were made with a JNM-FX100 (100 MHz) spectrometer (JEOL, Tokyo, Japan). Chemical shifts are reported in p.p.m. at room temperature using CDCl_3 as a solvent and tetramethylsilane as an internal standard. The thermal properties were examined by differential scanning calorimetry (TA3000: Mettler & Toledo, Columbus, OH, USA) and polarizing microscopic observation (BH-2: Nikon, Tokyo, Japan) with a Mettler FP900-FP82 (Mettler & Toledo). X-ray diffraction measurements of the smectic phases were performed using an X-ray diffractometer (Rint 2200: Rigaku, Tokyo, Japan) equipped with a hot stage (PM900: Linkam, Surrey, UK), using Ni-filtered $\text{Cu K}\alpha$ radiation.

RESULTS AND DISCUSSION

Phase transitions

The phase transitions were determined from the data obtained by differential scanning calorimetry, polarizing microscopic observation and X-ray diffraction measurements. The differential scanning calorimetry curves of P- n are shown in Figure 2. The phase transitions of P- n are summarized in Table 1 and Figure 3. P- n ($n = 2-12$) showed smectic phases such as smectic A, C and F phases upon heating and cooling. P-2, having the shortest spacer length, clearly formed a smectic A (SmA_2) phase with a bilayered structure, exhibiting a focal conic fan texture over a wide temperature range. P-3, P-4 and P-5 also exhibited the SmA_2 phase.

P-6 formed a smectic A (SmA_1) phase with a monolayered structure, in which the mesogenic side groups overlapped with one another. P-5 and P-6 showed a nematic phase with a schlieren texture, as well as the smectic A phase. The temperature range of the smectic

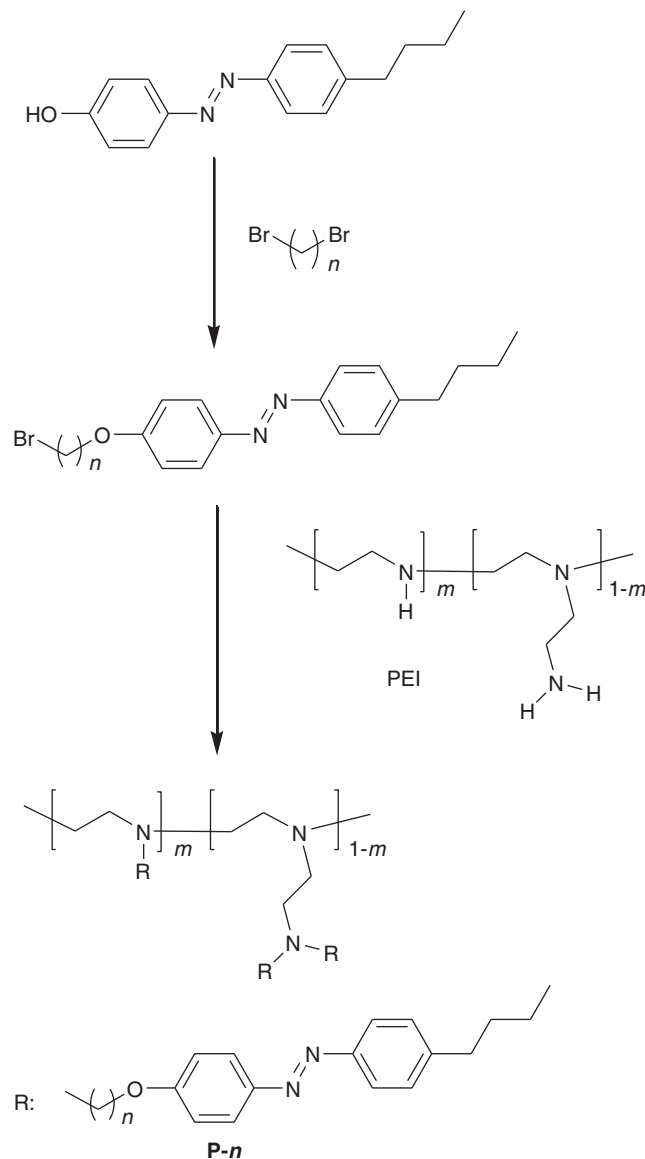


Figure 1 Synthetic scheme and structures of side-chain liquid crystal polymers (P- n ; $n = 2-12$) with branched polyethyleimineine backbones.

A phase of P-6 was the narrowest of all the P- n studied. P-7 also formed nematic and SmA_1 phases, whereas P-8 and P-9 showed nematic, SmA_1 , smectic C and smectic F phases. The smectic C phases appeared in a narrow temperature range. In P-10, P-11 and P-12, SmA_1 and smectic F phases were observed. The smectic F phase was formed by P- n with long spacer chains ($n = 8-12$). This indicates that a long spacer chain leads to the formation of a tilted smectic F phase, which is an ordered smectic phase. This is because the spacer chain acts to decouple the mesogenic groups from the polymer backbone, and this decoupling function becomes more effective with increasing spacer length.

Figure 4 shows the optical textures of P-8. Both schlieren mosaic and broken fan textures were observed in the smectic F phase. Upon heating the smectic F phase, both smectic schlieren and broken fan textures were obtained in the smectic C phase. In the smectic A phase, a focal conic fan texture and a perpendicular structure were formed. At the nematic-isotropic phase-transition point, droplets were

formed. The nematic and smectic optical textures of the other **P-*n*** resembled those of **P-8**. In the case of **P-*n*** with a smectic A–isotropic phase transition, batonnets were observed. The smectic orientations were maintained in the glass phase. The perpendicular structure (dark region in Figure 4) formed in the smectic A phase was characterized by an optical–uniaxial interference figure obtained by conoscopic observation.

The numbers in brackets in Table 1 indicate the phase-transition enthalpies. Table 2 shows the phase-transition entropies ($\Delta S(N-I)$,

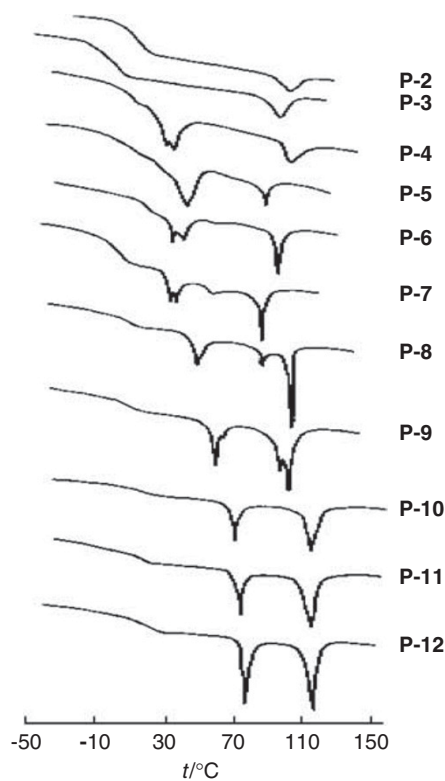


Figure 2 DSC curves of **P-*n*** on second heating.

$\Delta S(A-I)$, $\Delta S(A-N)$) obtained from the phase-transition enthalpies in Table 1. The enthalpies and entropies for the phase transition from the smectic A to the isotropic phase increased with increasing spacer chain length. A trend arose in which the even-membered **P-*n*** showed higher-transition enthalpies and entropies than the odd-membered **P-*n***, as shown in Figure 5. This even/odd effect of **P-*n*** for $n = 5-8$ was particularly remarkable. **P-6** exhibited the narrowest smectic A range. However, $\Delta S(A-N)$ and $\Delta S(A-N-I)$ of **P-6** were larger than those of **P-5** and **P-7**. This indicates that the orientational order of the smectic A phase in **P-6** is higher than in **P-5** and **P-7**. The phase-transition entropies (Table 2, $\Delta S(A-N-I)$) of **P-*n*** with $n = 10-12$ are approximately five to six times larger than those of **P-*n*** with $n = 2-4$. This indicates that an increase in the spacer chain length leads to an enhancement of the orientational order in the liquid crystalline state.

X-Ray diffraction measurements

In the smectic A phase, the X-ray diffraction pattern consists of sharp inner reflections and a broad outer reflection. The sharp inner reflections correspond to the smectic layer spacing, and the broad outer reflection indicates the absence of long-range order. The X-ray diffraction patterns in the smectic A phase of **P-4**, **P-6** and **P-11** are shown in Figures 6 and 7. The layer spacings are shown in Figure 8

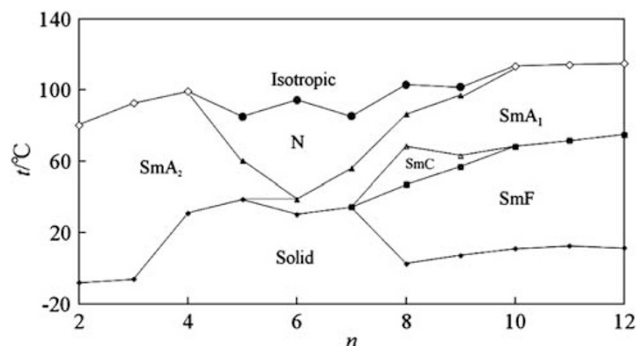


Figure 3 Phase transitions of **P-*n***: N, nematic; SmA_1 , monolayered smectic A; SmA_2 , bilayered smectic A; SmC, smectic C; and SmF, smectic F.

Table 1 Phase transition temperatures and phase transition enthalpies of **P-*n***

<i>n</i>	Phase transition temperatures/°C								
	T_g	T_{m1}	T_{m2}	T_{F-C}	T_{F-A}	T_{C-A}	T_{A-N}	T_{A-I}	T_{N-I}
2	-8.0	—	—	—	—	—	—	80.4(0.94)	—
3	-6.1	—	—	—	—	—	—	92.6(0.94)	—
4	4.8	24.6	31.2(1.23)	—	—	—	—	99.3(1.09)	—
5	7.0	22.7	38.9(2.77)	—	—	—	60.4(0.03)	—	85.0(0.66)
6	17.3	—	30.4(1.25)	—	—	—	39.0(0.99)	—	94.4(0.99)
7	1.0	31.3	34.6(0.47)	—	—	—	56.0(0.20)	—	85.3(0.94)
8	2.8	—	—	47.1	—	68.5	86.5(1.67)	—	103.0(2.12)
9	7.5	—	—	57.0	—	63.2	97.1(1.89)	—	101.7(1.89)
10	11.1	—	—	—	68.3(2.39)	—	—	113.5(5.13)	—
11	12.7	—	—	—	71.7(2.74)	—	—	114.3(5.30)	—
12	11.6	—	—	—	75.0(3.38)	—	—	114.9(6.02)	—

Abbreviations: T_{A-I} , smectic A–isotropic phase transition temperature; T_{A-N} , smectic A–nematic phase transition temperature; T_{C-A} , smectic C–A phase transition temperature; T_{F-A} , smectic F–A phase transition temperature; T_{F-C} , smectic F–C phase transition temperature; T_g , glass transition temperature; T_{m1} , solid–solid phase transition temperature; T_{m2} , solid–mesophase transition temperature; T_{N-I} , nematic–isotropic phase transition temperature.

Numbers in the brackets denote phase transition enthalpies in kJ mol^{-1} .

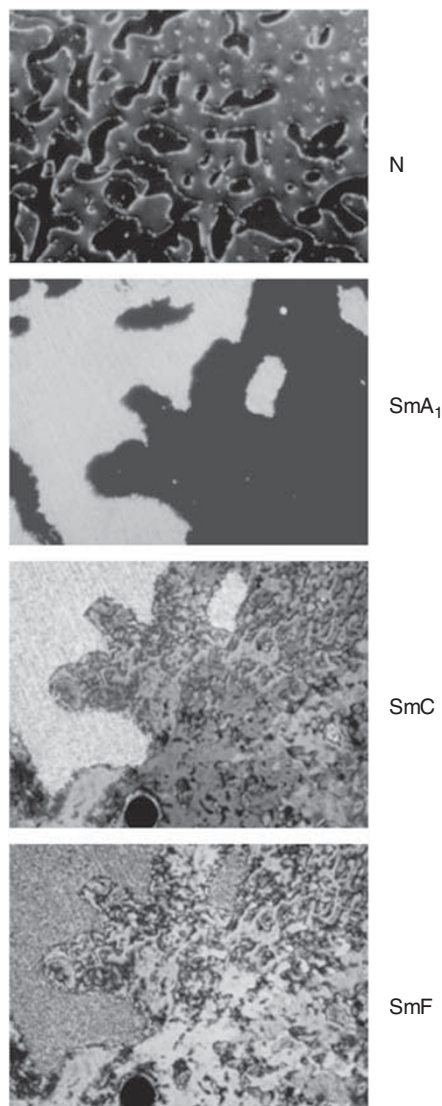


Figure 4 Optical textures of **P-8**. N: 92.5 °C, SmA₁: 72.0 °C, SmC: 60.0 °C and SmF: 45.0 °C.

Table 2 Phase transition entropies ($\text{JK}^{-1} \text{mol}^{-1}$) from smectic A to nematic phases

<i>n</i>	$\Delta S(A-I)$	$\Delta S(A-N)$	$\Delta S(N-I)$	$\Delta S(A-N-I)^a$
2	2.6	—	—	2.6
3	2.6	—	—	2.6
4	2.9	—	—	2.9
5	—	0.1	1.8	1.9
6	—	3.2	2.7	5.9
7	—	0.6	2.6	3.2
8	—	4.6	5.6	10.2
9	—	5.1	5.1	10.2
10	13.3	—	—	13.3
11	13.7	—	—	13.7
12	15.5	—	—	15.5

^aPhase transition entropy from smectic A to isotropic phases: $\Delta S(A-I)$ or sum of $\Delta S(A-N)$ and $\Delta S(N-I)$.

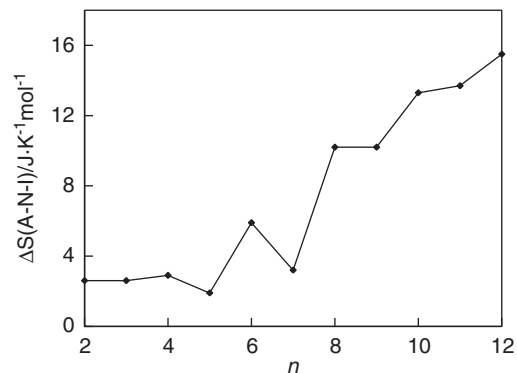


Figure 5 Transition entropies from smectic A to an isotropic phase for **P-*n***. In the case of **P-*n*** with $n=5-9$, $\Delta S(A-N-I)$ represents the sum of $\Delta S(N-I)$ and $\Delta S(A-N)$, which is shown in Table 3. The $\Delta S(A-N-I)$ of **P-*n*** with $n=2-4$ and $n=10-12$ corresponds to $\Delta S(A-I)$ in Table 3.

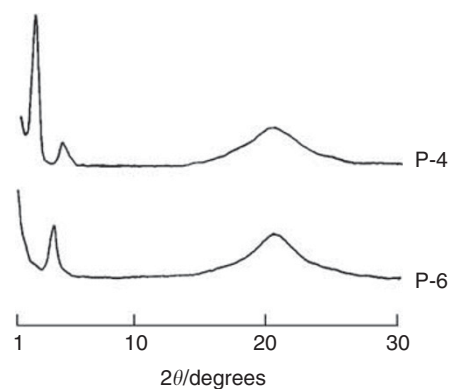


Figure 6 X-ray diffraction patterns of the smectic A phases of **P-4** (25 °C) and **P-6** (35 °C).

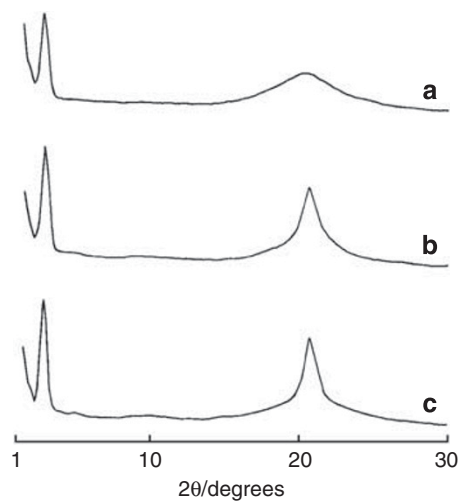


Figure 7 X-ray diffraction patterns of **P-11**: (a) SmA, 80 °C, (b) SmF, 65 °C and (c) SmF, 50 °C.

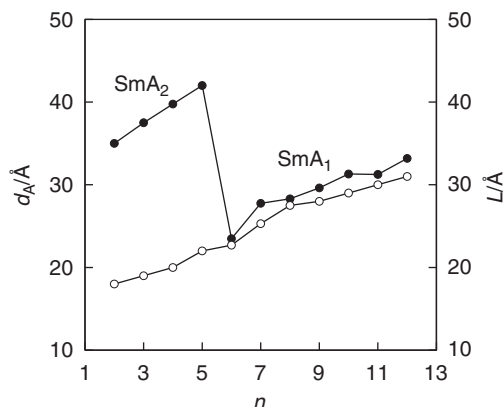


Figure 8 The layer spacings (d_A , filled circles) and extended lengths (L) of the mesogenic side groups (open circles) of **P-n**. In **P-n** with $n=2-5$, the layer spacing (bilayer) is twice the extended length of the mesogenic side group. In contrast, the layer spacing (monolayer) of **P-n** with $n=6-12$ corresponds to the extended length of the mesogenic side group.

Table 3 d -spacings of **P-n** with smectic F phase

Sample	d -spacing/Å		
	SmA	SmC	SmF
P-8	28.3 (75 °C)	27.4(61 °C)	26.3, 4.3 (57 °C)
P-9	29.6 (90 °C)	29.2(61 °C)	28.7, 4.3 (57 °C)
P-10	31.3 (100 °C)	—	30.2, 4.3 (60 °C)
P-11	31.8 (80 °C)	—	31.1, 4.3 (60 °C)
P-12	33.2 (100 °C)	—	34.2, 4.3 (60 °C)

and Table 3. The layer spacings (d_A) of the smectic A phase and the extended lengths (L) of the mesogenic side chains are summarized in Figure 8. **P-n** with $1 < n < 6$ showed the relationship $d_A \approx 2L$ in the smectic A phase. This indicates the formation of a bilayered structure in the smectic A phase (SmA₂), as shown in Figure 9. It is expected that a monolayered structure is formed in the smectic A phase (SmA₁) of **P-n** with $5 < n < 13$, where d_A corresponds to L , as shown in Figure 9. In the monolayered structure, the methylene spacer chains overlap with the butylazobenzene groups. The polymer backbones (PEI chains) and the mesogenic side groups aggregate, and, consequently, the smectic A layer consists of sublayers formed by the polymer backbones and mesogenic side groups. These two types of sublayers are piled alternately in the smectic phase. In addition, it is thought that the orientational order of the mesogenic side groups in the smectic A phases corresponds to the spacer chain length dependence of the transition entropies shown in Figure 5.

The X-ray diffraction patterns of the smectic C phase resembled those of the smectic A phase. In the case of the smectic F phase, a sharp outer reflection was observed as well as the sharp inner reflections (Figure 7; Table 3). The sharp outer reflection (4.3 Å) shows the formation of long-range order in the mesogenic side groups within the smectic F layers. The smectic C and F phases have a tilted monolayered structure, in which the mesogenic side groups are tilted toward the layer normal.

CONCLUSIONS

This research indicates that even when a side-chain liquid crystal polymer has a short spacer, a smectic phase may be formed stably

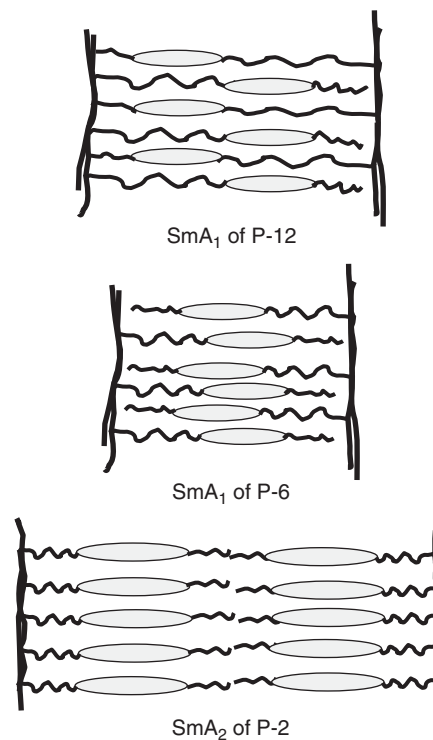


Figure 9 Possible packing models of smectic A phases. **P-n** with $n=2-5$ and **P-n** with $n=6-12$ formed the bilayered and monolayered smectic A structures, respectively.

Table 4 Liquid crystalline phases formed by **Br-n** monomers and **P-n** polymers

n	Br-n ^a	P-n
2	(N) ^b	SmA
3	No mesophase	SmA
4	N, SmA	SmA
5	N, SmA	N, SmA
6	N, SmA	N, SmA
7	N, SmA	N, SmA
8	No mesophase	N, SmA, SmC, SmF
9	SmA	N, SmA, SmC, SmF
10	(SmA) ^b	SmA, SmF
11	SmA	SmA, SmF
12	SmA	SmA, SmF

^a ω -bromo- α -(4-(4-(butyl)phenylazo)phenoxy)alkane.

^bMonotropic liquid crystalline phase.

over a wide temperature range and that a long spacer leads to the formation of tilted smectic phases. Furthermore, it is demonstrated that the balance of the spacer and mesogenic group is important for liquid crystal formation and the liquid crystal microstructure.

The **P-n** synthesized in this research formed smectic phases regardless of the spacer chain length (alkyl chain with n carbons ($n=2-12$)). **P-n** with $n=5-9$ exhibited the nematic phase. **P-6** showed the widest nematic range and the narrowest smectic range. The **P-n** with long spacer chains showed the smectic C and ordered smectic F phases, which are tilted smectic phases. Polymers with short spacers ($n=2-5$) showed different liquid crystal formation from

those with longer spacers ($n=6-12$). A short spacer allowed **P-*n*** to form a stable bilayered smectic A phase. With longer spacers, **P-*n*** had monolayered smectic A and tilted smectic phases. The thermal stability of the smectic phase was enhanced in **P-*n*** when the methylene spacer was short enough ($n=2-4$) or had a length similar to the length of the butylazobenzene mesogenic group ($n=10-12$). Furthermore, **P-*n*** revealed the nematic phase when the spacer was of medium length ($n=5-9$). This phase was not formed by **P-*n*** with $n=2-4$ or $n=10-12$. In particular, **P-6** exhibited a low smectic formation ability. **P-6** exhibited the nematic phase in the widest temperature range and the smectic phase in the narrowest temperature range. These results indicate that the liquid crystal formation, thermal stability of the smectic phase and liquid crystal microstructure strongly depend on the balance between the spacer length and the length of the butylazobenzene mesogenic group. Furthermore, the liquid crystalline properties of **P-*n*** are different from those of the monomers (**Br-*n***: ω -bromo- α -(4-(4-(butyl)phenylazo)phenoxy)alkane) corresponding to the mesogenic side groups of **P-*n***, as shown in Table 4. **Br-*n*** with $n=4-7$ exhibited nematic and smectic A phases, and **Br-*n*** with $n=3$ and 8 did not show a liquid crystalline phase. Additionally, **Br-*n*** with $n=9-12$ revealed a smectic A phase, and **Br-2** formed a nematic phase. For $n=2-4$ and 8-12, **P-*n*** exhibited completely different liquid crystal formation from **Br-*n***. This difference is due to the influence of the polymer backbone. In addition, **P-*n*** with $n=8-12$ formed the tilted smectic phases (smectic C and F phases), which were not exhibited by **Br-*n***. The combination of the polymer backbone and the spacer is useful for controlling the liquid-crystalline orientation of the

mesogenic groups. The results of this research can be effectively applied to the design of future liquid crystal polymers.

- 1 Zentel, R. & Ringsdorf, H. Synthesis and phase behavior of liquid crystalline polymers form chloroacrylates and methacrylates. *Makromol. Chem. Rapid Comm.* **5**, 393-398 (1984).
- 2 Shibaev, V. P., Kostromin, S. G. & Plate, N. A. Thermotropic liquid-crystalline polymers-VI: comb-like liquid-crystalline polymers of the smectic and nematic types with cyanobiphenyl groups in the side-chain. *Eur. Poly. J.* **18**, 651-659 (1982).
- 3 Mauzac, M., Hardouin, F., Richard, H., Achard, M. F., Sigaud, G. & Gasparoux, H. Effect of the chemical constitution of the side-chain on the formation and the structure of mesophases in some polysiloxanes. *Eur. Polym. J.* **22**, 137-142 (1986).
- 4 Plate, N. A. & Shibaev, V. P. in *Comb-Shaped Polymers and Liquid Crystals* (eds Plate, N. A. & Shibaev, V. P.) Ch. 4 199-359 (Plenum Press, New York, 1987).
- 5 Ujiie, S., Yano, Y. & Mori, A. Thermal and liquid crystalline properties of a polymer with amphiphilic-mesogenic side-chain. *Mat. Res. Soc. Symp. Proc.* **709**, 135-140 (2002).
- 6 Yano, Y., Ujiie, S. & Mori, A. Phase transitions of side chain liquid crystal polyamines. *Mol. Cryst. Liq. Cryst.* **365**, 255-262 (2001).
- 7 Ujiie, S., Tanaka, Y. & Imura, K. Thermal and liquid crystalline properties of polymethacrylates with ammonium units and their non-ionic family. *Polym. Adv. Technol.* **11**, 450-455 (2000).
- 8 Ujiie, S., Maekawa, K., Tsukamoto, S. & Imura, K. Phase transitions of liquid crystalline comb-shaped polymers having azo dye units. *Sen'i Gakkaishi* **56**, 95-97 (2000).
- 9 Percec, V. & Pugh, C. in *Side Chain Liquid Crystal Polymers* (ed. McArdle, C. B.) Ch. 3 31-105 (Blackie, New York, 1989).
- 10 Finkelmann, H., Ringsdorf, H. & Wendorff, J. H. Model consideration and examples of enantiotropic liquid crystalline polymers. *Makromol. Chem.* **179**, 273-276 (1978).
- 11 Ujiie, S. & Imura, K. Formation of smectic orientational order in an ionic thermotropic liquid-crystalline side-chain polymer. *Polym. J.* **25**, 347-354 (1993).
- 12 Ujiie, S. & Imura, K. Ammonium halide type thermotropic liquid-crystalline polyethyleneimine and those low-mass model compounds. *Chem. Lett.* 995-998 (1990).